Composites Communications 44 (2023) 101752

Contents lists available at ScienceDirect

Composites Communications

journal homepage: www.elsevier.com/locate/coco

Sequential multi-material embedded 3D printing of soft composite actuators

Zhenhua Wang [a,b], Jingze Wang [b,e], Jizhe Wang [a,d], Boyu Zhang [c,d,e], Yuan Yao [c,d,e], Nanjia Zhou [c,d,e,**], Weicheng Cui [b,e,*]

[a] Zhejiang University, Hangzhou, Zhejiang, 310027, China
[b] Key Laboratory of Coastal Environment and Resources of Zhejiang Province, School of Engineering, Westlake University, Hangzhou, Zhejiang, 310030, China
[c] Research Center for Industries of the Future, Westlake University, Hangzhou, Zhejiang, 310030, China
[d] Key Laboratory of 3D Micro/nano Fabrication and Characterization of Zhejiang Province, School of Engineering, Westlake University, Hangzhou, Zhejiang, 310030, China
[e] Institute of Advanced Technology, Westlake Institute for Advanced Study, Hangzhou, Zhejiang, 310024, China

ARTICLE INFO

Keywords:
3D printing
Soft robot
Composite actuator
Soft sensor

ABSTRACT

Soft composite actuators are developed for a variety of applications, yet the fabrication of composite actuators with complex external geometries and internal structures such as self-sensing actuators remains one of the greatest impediments. Here, the limitation is addressed by a novel 3D printing technology, Sequential Multi-material Embedded 3D Printing (SME3P). Different properties of printed inks are investigated to optimize the fabrication of soft composite actuators. Various composite sensors and actuators are fabricated to verify the feasibility of SME3P. This SME3P technique offers an unparalleled printing capability to fabricate the complex composite actuators for real-life applications.

1. Introduction

Soft composite actuators have emerged as pivotal components in diverse fields such as space and deep-sea exploration [1–4], wearable technology [5], biomedical engineering [6], and others. The inherent complexities in the geometries and functionalities of composite actuators with mechanical and electrical properties make them particularly challenging to fabricate. This difficulty, however, is being assuaged by the advent of additive manufacturing (3D printing). 3D printing promises to revolutionize traditional manufacturing processes of composites that are both time-consuming and labor-intensive [7]. Nevertheless, the traditional layer-by-layer printing process results in limited printing shape [8,9]. Recently, 4-axis printing has been applied in the fabrication of soft composite actuators. This method is effective in the fabrication of tubular based structures, while it is hard to fabricate actuators in other shapes [10–12]. An emerging solution to these limitations is embedded 3D printing (E3P), an adaptation of the traditional 3D printing method. E3P has seen a surge in popularity due to its potential for freeform printing, enabled by the use of a suspension medium to uphold the printed structures [13]. E3P has already been successfully employed in the construction of various sensors and actuators [14–18], yet very few instances of integrated sensors and actuators have been reported. Truby et al. made headway in this field when they utilized sacrificial ink (Pluronic F127) to develop air channels and conductive ink (ionic gel) to fabricate sensors via a modified E3P method [19]. However, the reach of this method is constrained by the acrylic mold that limits the actuator's external geometry, thereby precluding the production of complex external shapes for soft actuators, such as those seen in composite-reinforced actuators.

In this work, we report a method to integrate sensors into composite actuators via sequential multi-materials embedded 3D printing (SME3P). The rheological, mechanical, and electrical properties of printed ink is investigated to optimize the fabrication and design of soft actuators. The resistive and capacitive sensors are fabricated to verify SME3P's ability of integrating sensors into soft matric materials. At last, the self-sensing soft actuators is printed to demonstrate SME3P's potential to be a versatile platform for the future fabrication of soft self-sensing robots.

* Corresponding author. Key Laboratory of Coastal Environment and Resources of Zhejiang Province, School of Engineering, Westlake University, Hangzhou, Zhejiang, 310030, China.
** Corresponding author. Research Center for Industries of the Future, Westlake University, Hangzhou, Zhejiang, 310030, China.
E-mail addresses: zhounanjia@westlake.edu.cn (N. Zhou), cuiweicheng@westlake.edu.cn (W. Cui).

https://doi.org/10.1016/j.coco.2023.101752
Received 13 August 2023; Received in revised form 10 October 2023; Accepted 11 October 2023
Available online 13 October 2023

2. Results and discussion

2.1. Sequential multi-materials embedded 3D printing (SME3P)

Take the printing of a self-sensing composite reinforced actuator as an example, SME3P involves several separate printing stages (Fig. 1A). First, the inflating body is printed in the matrix using elastomer ink. Second, sensors are printed into the first printed inflating body via conductive ink. In this stage, the first printed structure functions as the matrix in E3P. Finally, the reinforced composite is conformally printed on and/or into the inflating body to limit undesired deformation. The structure of our printing system is shown in Fig. 1B.

2.2. Rheological and electrical properties of inks

First, the conductive ink was prepared by composing an uncured silicone matrix Ecoflex 0030 (Eco30) and hydrophobic carbon black (CB), which serves as both the rheological modifier and conductive filler. The extrusion process of the SME3P requires the ink to have shear-thinning property and proper yield stress [20]. As the carbon black loading increases from 1 to 2.5 wt%, all inks exhibit shear-thinning behavior (Fig. 2A). However, only inks with more than 1.5 wt% CB exhibits yield stress fluid properties (Fig. 2B), making them suitable for 3D printing. The conductive inks show tradeoff between mechanical and electrical properties. The conductivity of the conductive ink should be as high as possible under the premise of curability. Dog-bone-shaped tensile test samples were fabricated for mechanical testing (**Figrue S1**). As concentrations of CB increases from 1 to 2.5 wt%, the elastic modulus (at 10 % strain) of the cured conductive ink decreases from 76 kPa to 15.5 kPa, and the tensile strength from 550 kPa to 97 kPa, respectively (Fig. 2C). The addition of CB slows the curing velocity of conductive inks [21]. More than 3 wt% of CB makes the conductive ink unable to cure within the matrix. Similar phenomenon has been reported in other works [22]. As the loading of CB increased to 2.5 wt%, the conductivity of the cured ink rises to 0.344 S/cm, and the resistivity decreased to 2.9 Ω cm, respectively (Fig. 2D). After a comprehensive consideration of the tradeoff between rheological, electrical, and mechanical properties, 2.5 wt% was chosen as the final concentration of the CB. The added CBs are dispersed in the conductive ink in the form of particles with diameters ranging from several to 50 μm (Fig. S2).

As reported in previous work, the plateau storage moduli (G′) of inks utilized in embedded printing should be orders of magnitude higher than those of the matrix [23]. The rheological properties of the hard and soft inks have been studied in our previous work [24]. The G' of the matrix and inks in our work are shown in Fig. 2E, satisfying the aforementioned criterion. For better reinforcement performance, the elastic modulus (E) of hard ink should be much higher than that of the soft ink. Therefore, Ecoflex 0030 (E = 76 kPa) were chosen as the soft ink, and carbon fiber reinforced Slygard 184 was chosen as the hard ink (E = 7000 kPa), ensuring desired pneumatic responses of our printed actuators (Fig. 2F). The curing time of hard, conductive, and soft ink were 4,4, and 3 h at 80 °C, respectively.

2.3. Characterization of single sensor performance

Upon the design of inks and matrix materials, a soft resistive strain sensor was printed. An elastomer sheet was first printed using soft ink within the matrix. Subsequently, a resistive sensor, with a linewidth of 600 μm was printed into the elastomer using conductive ink. The optimization of printing parameters is shown in Supplementary Information (Fig. S3), and final printing parameters are listed in Table S2. The resistance of the cured sensor (R_0) is approximately 350 kΩ. We evaluated the electrical performance of the sensor under tensile strain (1 mm/s). As the linear strain escalated to 300 %, the normalized R/R_0 increased to 7, before failing at a strain of ~320 % (Fig. 3A). At a strain of 200 %, the sensor demonstrated linearity with a gauge factor of around 2. The discrepancy between the loading and unloading curve reveals the hysteresis of the strain sensor (Fig. 3B), primarily attributed to the energy dissipation of the conductive particle networks [25]. Efforts can be made to develop low hysteresis materials as the conductive ink. A cycling loop test was conducted under a smaller strain (100 %). R/R_0 stabilized at approximately 2.7 in the final 50 cycles (Fig. S4), indicating the sensor's good reliability under small strain.

Another type of soft sensor, capacitive sensor was also fabricated via SME3P (**Supplementary video 1**). Two plates were printed into the first printed elastomer sheet, which serves as both package and dielectric layer. The plates have a thickness of 600 μm. The distance between plate was 250 μm (Fig. 3C). The capacitance of the cured capacitive sensor was measured as 1.28 pF. A platform was established to characterize the tactile sensing ability of the printed capacitive sensor (Fig. 3C). As the loading displacement increased from 0 to 500 μm, the normalized C/C_0 rose to approximately 1.4 (Fig. 3D). Compared to the strain sensor, the capacitive sensor shows lower hysteresis. Cycle testing was conducted (with a displacement of 400 μm) to assess the stability of the sensor. In

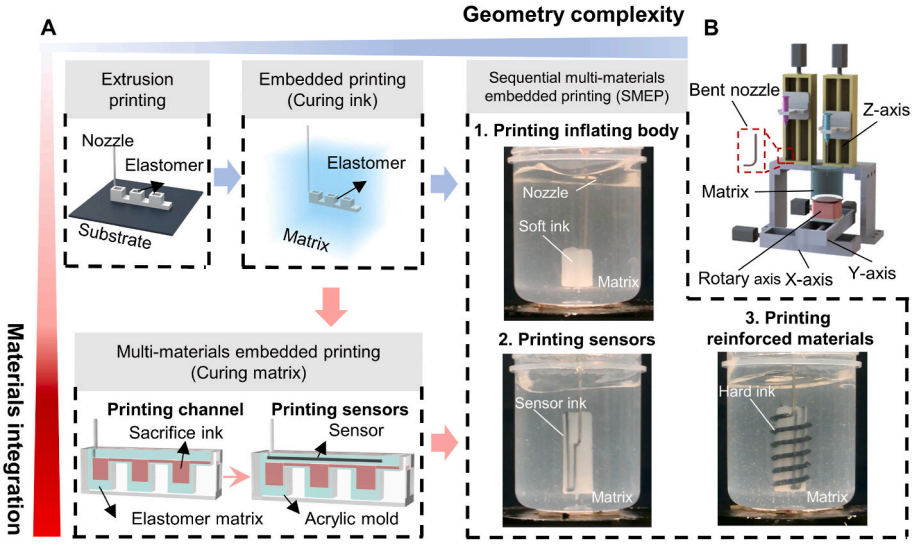

Fig. 1. Sequential multi-materials embedded 3D printing (SME3P): (A) Adapted from embedded printing, SME3P involves three steps to integrate sensors into soft reinforced actuators; (B) Set up of our SME3P platform.

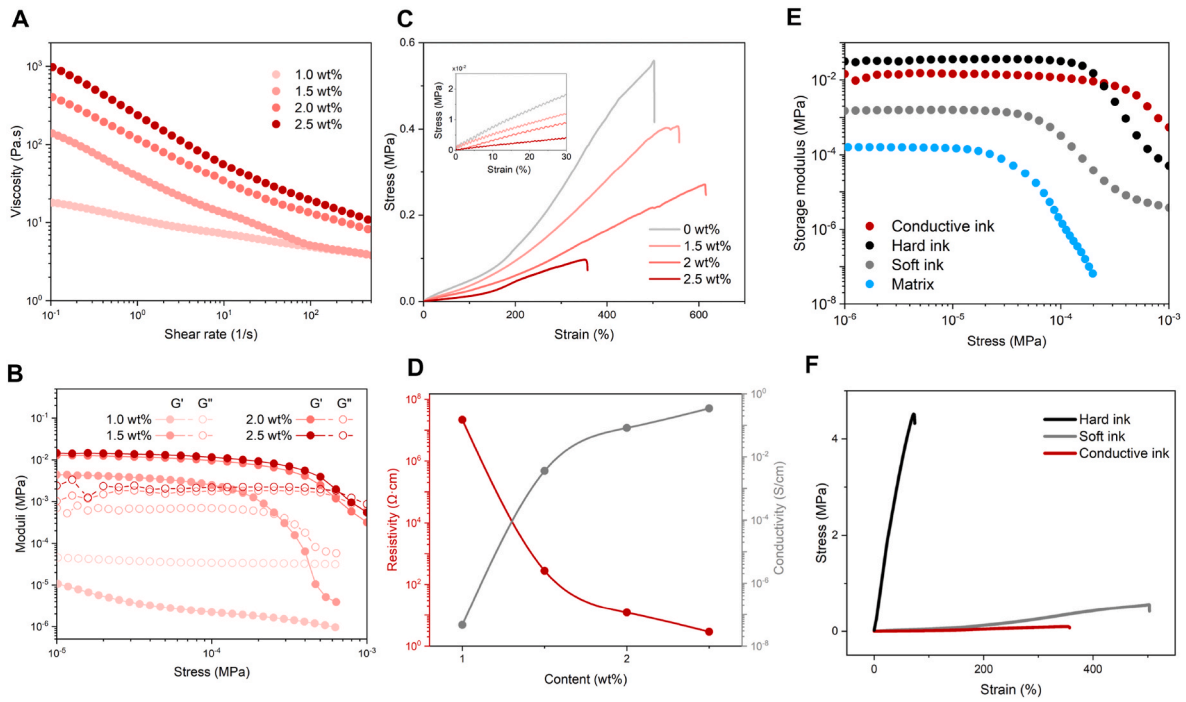

Fig. 2. Ink properties: (A) Viscosity of conductive inks as a function of shear rate with different carbon black loadings (B) Storage moduli (G′) and loss moduli (G″) of conductive inks as a function of shear rate with different carbon black loadings; (C)Stress-strain curve of cured conductive ink with different carbon black loadings; (D) Conductivity and resistivity of conductive ink with different carbon black loadings; (E) Comparison between the plateau storage of matrix and different inks; (F) Stress-strain curve of three different cured inks.

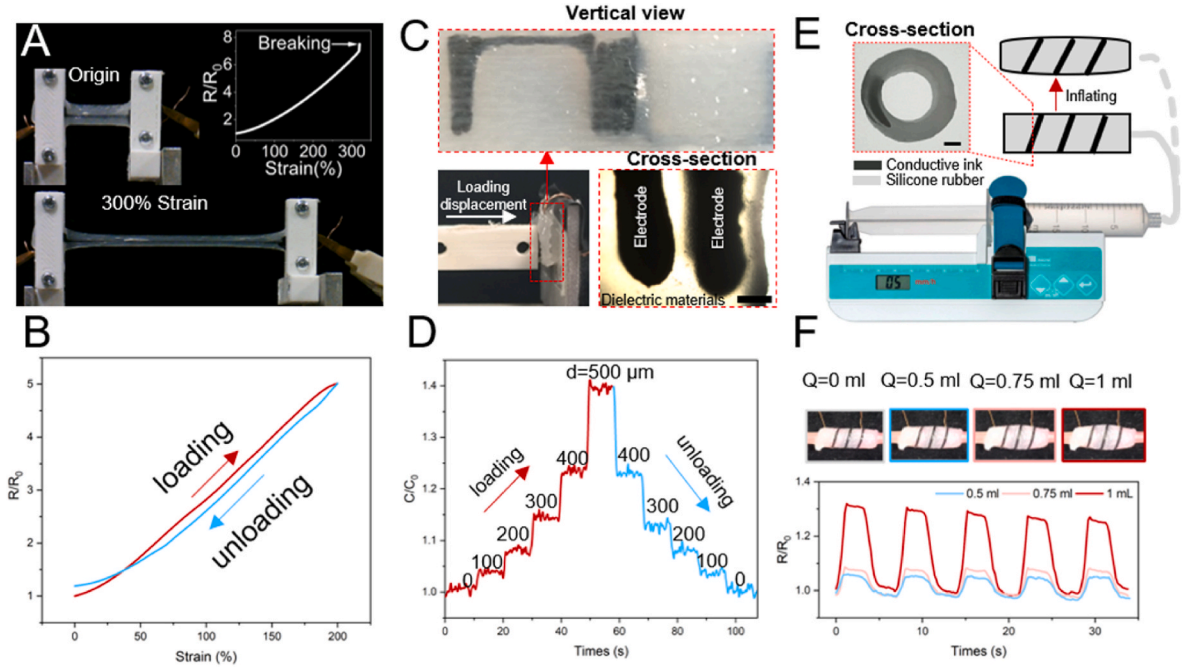

Fig. 3. Characterization of printed sensors: (A) Tensile testing of the printed resistive sensor; (B) The loading and unloading resistive change with the strain of 200 %; (C) Cross-section (Scale bar: 500 μm) and testing platform of capacitive sensor; (D) The loading and unloading curves of capacitive change with a loading displacement of 500 μm; (F) Cycle testing of the capacitive sensor with a loading displacement of 400 μm; (E) Cross-section (Scale bar: 200 μm) and testing platform of tubular sensor; (F) The resistive change as the tubular sensor inflated by 0.5, 0.75, and 1 ml air.

comparison to the resistive sensor, the soft capacitive sensor demonstrated poor stability over 200 cycles (Fig. S5). This instability is mainly due to the large initial resistance and the change in resistance of the electrodes when the capacitive sensor is pressed. The stability can be enhanced by using highly conductive ink to print the electrodes.

Since the external shape of the first printing via SME3P isn't limited by the mold, a tube-shaped resistive sensor was fabricated. A helical resistive senor was printed into the tube wall (Fig. 3E). An injection pump was used to inflate the tube sensor. Upon 0.5 ml, 0.75 ml, and 1 ml of air were injected to the sensor, the respective R/R_0 values increased to

1.04, 1.08, and 1.31 (Fig. 3F). The tube sensor demonstrated stable performance in a cycling test with an inflation volume of 1 ml (Fig. S6).

2.4. Characterization of printed actuators with embedded sensors

Encouraged by the successful printing of basic sensors, self-sensor composite reinforced actuators were fabricated via SME3P by printing constraining fibers on the surface of tubular shape sensors. A bender was first printed as a demonstration in three steps. The actuator measures 30 mm in length, with a diameter and wall thickness of 10 mm and 2 mm, respectively (Fig. 4A). A U-shape resistive sensor (R_0 = 330 kΩ) with linewidth of 800 μm was printed into the wall. Different materials in the printed actuator are bonded by Si–*O*–Si bonds (Fig. S7). The actuator will bend rightwards upon inflating because of the structural asymmetry (Fig. 4A). As the inflating pressure increasing from 0 to 13 kPa, the bending angle reaches 53°, and R/R_0 increases to 6.46 (Fig. 4B). Both the bending angle and the normalized resistance exhibit hysteresis due to the inherent hysteresis in the silicone rubbers used. In a cycling tensile test run at an inflating pressure of 8 kPa, the normalized resistance (R/R_0) of the sensors slightly decreased from 2 to 1.7 within the first 50 cycles, but held steady thereafter (Fig. 4C).

A bidirectional bender with more complex inner channels was printed for the last demonstration (**Supplementary video 2**). Two inflating channels were arranged in the actuator, and two sensors were embedded into the outer walls of inflating channels (Fig. 4D, left). Inflating either channel of the bidirectional bender prompts it to bend in the opposite direction, whereas simultaneous inflation of both channels extends the actuator axially (Fig. 4D, right). Upon the left channel was inflated by 20 kPa, the actuator bent rightwards in the angle of ~55°, R/R_0 values of left and right sensor were 5.1 and 1.74 (Fig. S8). When the right channel was inflated, the bending angle reached 63° (Fig. S9), with corresponding R/R_0 value of 1.57 (left) and 3.50 (right). The asymmetry may be caused by the relatively imprecise nature of E3P [13], an aspect that warrants further refinement. When both channels were inflated, the actuator extended by ~27 %. Unlike single-direction bending, R/R_0 values of both sensors surged to 4.5 and 3.77, respectively (Fig. S10). When two channels were inflated and deflated sequentially (Fig. 4D, bottom), the response of actuator can be recognized by analyzing the changes in the R/R_0 values of the two sensors (Fig. 4E, up).

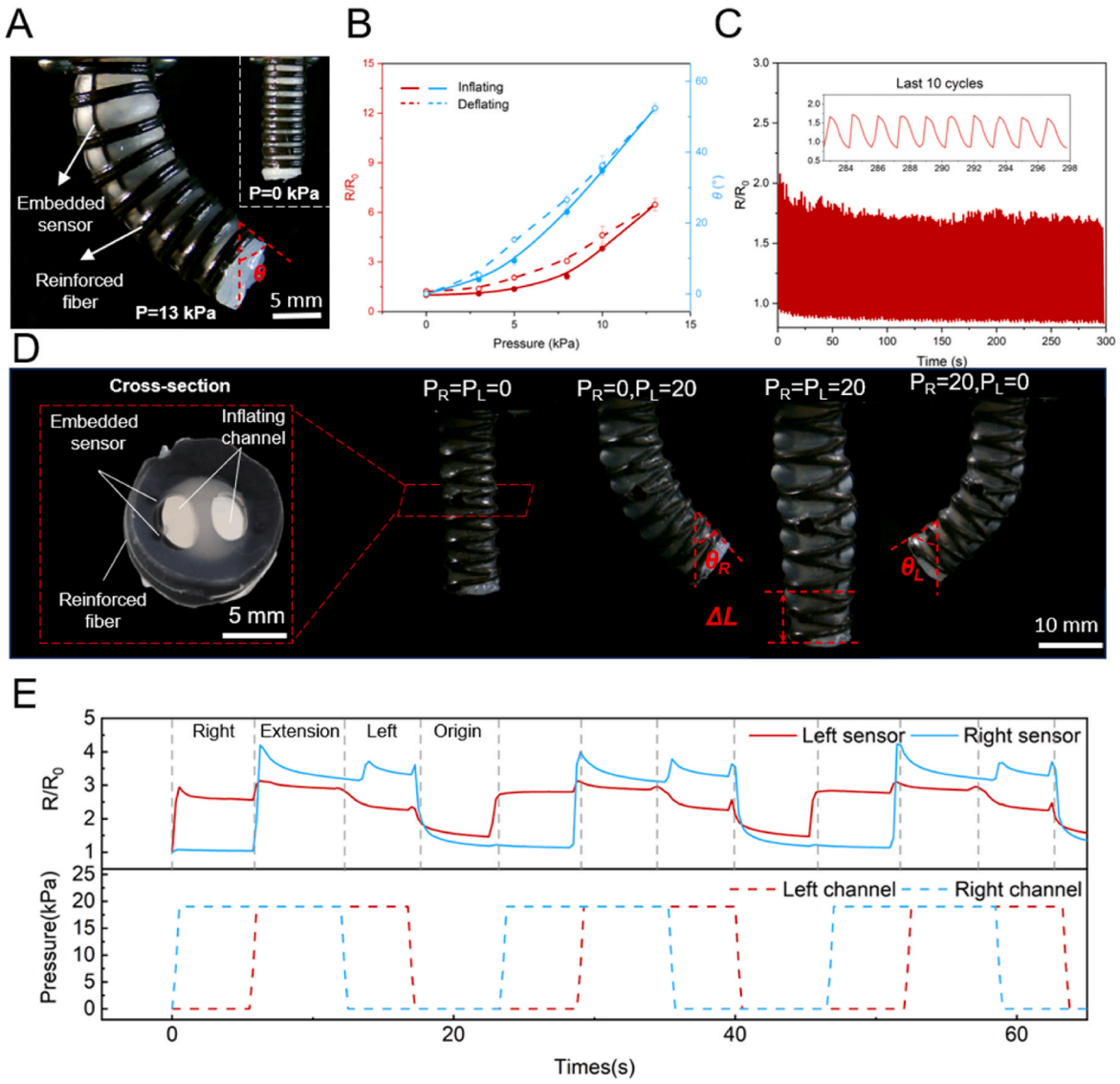

Fig. 4. Characterization of printed actuators: (A) Printed bender inflated by 13 kPa; (B) Bending angle (θ) and normalized resistance (R/R_0) of the actuator inflated by different pressures; (C) Cycling test of the bender in the inflating pressure of 8 kPa; (D) Structure of printed bidirectional bender and its pneumatic responses in different inflating conditions; (E) Comparison of the R/R_0 values of two sensors when the channels were inflated and deflated sequentially.

3. Conclusion

In this work, we have introduced a novel method (SME3P) to fabricate self-sensing composite-reinforced actuators. Properties of ink and matrix have been studied to ensure the successful printing. Different sensors and actuators in planer and tubular shapes have been fabricated to show the feasibility of SME3P to integrate sensors into soft robots. The SME3P can be easily extended to fabricate other composite devices rapidly (i.e., wearable electronics), in which functional composites need to be embedded into matrix materials for practical applications.

CRediT authorship contribution statement

Zhenhua Wang: Investigation, Data curation, Methodology, Writing – original draft. **Jingze Wang:** Investigation, Data curation, Methodology. **Jizhe Wang:** Investigation, Data curation. **Boyu Zhang:** Formal analysis, Methodology. **Yuan Yao:** Formal analysis, Methodology. **Nanjia Zhou:** Conceptualization, Supervision, Writing – review & editing. **Weicheng Cui:** Conceptualization, Supervision, Writing – review & editing.

Declaration of competing interest

The authors declare that they have no known competing financial interests or personal relationships that could have appeared to influence the work reported in this paper.

Data availability

Data will be made available on request.

Acknowledgement

The authors are grateful for the financial support for this research by the National Key Research and Development Program (2022YFC2805200), Research center for industries of the Future (RCIF), the National Natural Science Foundation of China (No. 51905446), Scientific Research Funding Project of Westlake University (2021WUFP017), and the Startup funding of New-joined PI of Westlake University (041030150118).

Appendix A. Supplementary data

Supplementary data to this article can be found online at https://doi.org/10.1016/j.coco.2023.101752.

References

[1] Y. Zhang, P. Li, J. Quan, L. Li, G. Zhang, D. Zhou, Progress, challenges, and prospects of soft robotics for space applications, Advanced Intelligent Systems 5 (3) (2023), 2200071.
[2] G. Li, X. Chen, F. Zhou, Y. Liang, Y. Xiao, X. Cao, et al., Self-powered soft robot in the mariana trench, Nature 591 (7848) (2021) 66–71.
[3] Z. Wang, W. Cui, For safe and compliant interaction: an outlook of soft underwater manipulators, Proc. IME M J. Eng. Marit. Environ. 235 (1) (2021) 3–14.
[4] Soft robots for ocean exploration and offshore operations: a perspective, Soft Robot. 8 (6) (2021) 625–639.
[5] F. Connolly, D.A. Wagner, C.J. Walsh, K. Bertoldi, Sew-free anisotropic textile composites for rapid design and manufacturing of soft wearable robots, Extreme Mechanics Letters 27 (2019) 52–58.
[6] M. Cianchetti, C. Laschi, A. Menciassi, P. Dario, Biomedical applications of soft robotics, Nat. Rev. Mater. 3 (6) (2018) 143–153.
[7] S. Park, W. Shou, L. Makatura, W. Matusik, K. Fu, 3D printing of polymer composites: materials, processes, and applications, Matter 5 (1) (2022) 43–76.
[8] M. Schaffner, J.A. Faber, L. Pianegonda, P.A. Rühs, F. Coulter, A.R. Studart, 3D printing of robotic soft actuators with programmable bioinspired architectures, Nat. Commun. 9 (1) (2018) 878.
[9] P. Zhang, I.M. Lei, G. Chen, J. Lin, X. Chen, J. Zhang, et al., Integrated 3D printing of flexible electroluminescent devices and soft robots, Nat. Commun. 13 (1) (2022) 4775.
[10] M. Mohammadi, A.Z. Kouzani, M. Bodaghi, Y. Xiang, A. Zolfagharian, 3D-Printed phase-change artificial muscles with autonomous vibration control, Advanced Materials Technologies (2023), 2300199 n/a(n/a).
[11] A. Zolfagharian, M. Lakhi, S. Ranjbar, M. Sayah Irani, M. Nafea, M. Bodaghi, 4D printing parameters optimisation for bi-stable soft robotic gripper design, J. Braz. Soc. Mech. Sci. Eng. 45 (4) (2023) 224.
[12] A. Zolfagharian, S. Gharaie, A.Z. Kouzani, M. Lakhi, S. Ranjbar, M. Lalegani Dezaki, et al., Silicon-based soft parallel robots 4D printing and multiphysics analysis, Smart Mater. Struct. 31 (11) (2022), 115030.
[13] J. Zhao, N. He, A mini-review of embedded 3D printing: supporting media and strategies, J. Mater. Chem. B 8 (46) (2020) 10474–10486.
[14] T. Calais, N.D. Sanandiya, S. Jain, E.V. Kanhere, S. Kumar, R.C.-H. Yeow, et al., Freeform liquid 3D printing of soft functional components for soft robotics, ACS Appl. Mater. Interfaces 14 (1) (2022) 2301–2315.
[15] B. Herren, M.C. Saha, M.C. Altan, Y. Liu, Development of ultrastretchable and skin attachable nanocomposites for human motion monitoring via embedded 3D printing, Compos. B Eng. 200 (2020), 108224.
[16] Z. Wang, B. Zhang, W. Cui, N. Zhou, Freeform fabrication of pneumatic soft robots via multi-material jointed direct ink writing, Macromol. Mater. Eng. 307 (4) (2022), 2100813.
[17] Y. Hui, Y. Yao, Q. Qian, J. Luo, H. Chen, Z. Qiao, et al., Three-dimensional printing of soft hydrogel electronics, Nature Electronics 5 (12) (2022) 893–903.
[18] Y. Yao, Y. Hui, Z. Wang, H. Chen, H. Zhu, N. Zhou, Granular ionogel particle inks for 3D printed tough and stretchable ionotronics, Research 6 (2023), 0104.
[19] R.L. Truby, M. Wehner, A.K. Grosskopf, D.M. Vogt, S.G.M. Uzel, R.J. Wood, et al., Soft somatosensitive actuators via embedded 3D printing, Adv. Mater. 30 (15) (2018), 1706383.
[20] R.L. Truby, J.A. Lewis, Printing soft matter in three dimensions, Nature 540 (7633) (2016) 371–378.
[21] H. Devaraj, K. Yellapantula, M. Stratta, A. McDaid, K. Aw, Embedded piezoresistive pressure sensitive pillars from piezoresistive carbon black composites towards a soft large-strain compressive load sensor, Sensor Actuator Phys. 285 (2019) 645–651.
[22] J. Wang, Q. Li, C. Wu, H. Xu, Thermal conductivity and mechanical properties of carbon black filled silicone rubber, Polym. Polym. Compos. 22 (4) (2014) 393–400.
[23] A.K. Grosskopf, R.L. Truby, H. Kim, A. Perazzo, J.A. Lewis, H.A. Stone, Viscoplastic matrix materials for embedded 3D printing, ACS Appl. Mater. Interfaces 10 (27) (2018) 23353–23361.
[24] Z. Wang, B. Zhang, Q. He, H. Chen, J. Wang, Y. Yao, et al., Multimaterial embedded 3D printing of composite reinforced, Soft Actuators. Research. 6 (2023), 0122.
[25] J. Shintake, Y. Piskarev, S.H. Jeong, D. Floreano, Ultrastretchable strain sensors using carbon black-filled elastomer composites and comparison of capacitive versus resistive sensors, Advanced Materials Technologies 3 (3) (2018), 1700284.
CRediT authorship contribution statement.